

Nanoscale

Accepted Manuscript



This is an *Accepted Manuscript*, which has been through the Royal Society of Chemistry peer review process and has been accepted for publication.

Accepted Manuscripts are published online shortly after acceptance, before technical editing, formatting and proof reading. Using this free service, authors can make their results available to the community, in citable form, before we publish the edited article. We will replace this *Accepted Manuscript* with the edited and formatted *Advance Article* as soon as it is available.

You can find more information about *Accepted Manuscripts* in the [Information for Authors](#).

Please note that technical editing may introduce minor changes to the text and/or graphics, which may alter content. The journal's standard [Terms & Conditions](#) and the [Ethical guidelines](#) still apply. In no event shall the Royal Society of Chemistry be held responsible for any errors or omissions in this *Accepted Manuscript* or any consequences arising from the use of any information it contains.

ARTICLE

Interplay between quantum interference and conformational fluctuations in single-molecule break junctions

Cite this: DOI: 10.1039/x0xx00000x

Marco Berritta^{a†}, David Zs. Manrique^{b†}, Colin J. Lambert^b

Received 00th January 2012,

Accepted 00th January 2012

DOI: 10.1039/x0xx00000x

www.rsc.org/

We theoretically explored the combined role of conformational fluctuations and quantum interference in determining the electrical conductance of single-molecule break junctions. In particular we computed the conductance of a family of methylsulfide-functionalized trans- α,ω -diphenyloligoenes molecules, with terminal phenyl rings containing meta or para linkages, for which (at least in the absence of fluctuations) destructive interference in the former is expected to decrease their electrical conductance compared with the latter. We compared the predictions of density functional theory (DFT), in which fluctuational effects are absent, with results for the conformationally-averaged conductance obtained from an ensemble of conformations obtained from classical molecular dynamics. We found that junctions formed from these molecules exhibit distinct transport regimes during junction evolution and the signatures of quantum interference in these molecules survive the effect of conformational fluctuations. Furthermore, the agreement between theory and experiment is significantly improved by including conformational averaging.

Introduction

Although the dream of utilising quantum interference (QI) effects in single molecules has been discussed for many years¹, experimental indications of room-temperature QI in electron transport through single molecules were obtained only recently²⁻¹⁹. In all of the above cases, evidence of QI was obtained by comparing theory with experiment and in some cases by comparing the conductances across families of related molecules. QI can manifest itself as both destructive and constructive interference, leading to molecules with anomalously-low or high electrical conductances respectively. For example in^{3, 7, 8, 11} destructive QI is signalled by the appearance of a Fano resonance in molecular wires with cross-conjugated sub-units, leading to suppression of their electrical conductance. Molecular systems exploiting destructive QI are predicted to exhibit huge thermoelectric conversion efficiencies, potentially exceeding those of commercially-available materials. Other manifestations of QI occur when one molecule is contacted to another in a phase-coherent manner¹⁴, which again leads to an enhancement of thermoelectric performance, or when sub-units of a molecule are systematically rotated^{2, 3, 16, 17, 19} to break conjugation or engineer the positions of transport resonances. Theoretical analyses of QI in molecular junctions typically focus on idealised junction geometries and molecular conformations, whereas configuration

changes within junctions or within the sub-units of molecules can affect the conductance by orders of magnitude²⁰, which is why experimental measurements of conductance invariably rely on statistical analyses of conductance histograms. The aim of this paper is to address this disconnect between theory and experiment by investigating the interplay between fluctuations and QI.

In ref²¹ it was shown that due to thermal fluctuations, molecules can explore several conformations leading to a decrease of the measured conductance. In ref²²⁻²⁴ thermally-induced conformational fluctuations were responsible for the detachment of the backbone part of the molecule from the electrodes, leading to the appearance of multiple peaks in conductance histograms. In particular, in the case where the anchor groups at the ends of the backbone are aromatic rings, it was shown that the conductance of the junction can be switched by geometrically constraining conformations to either favour or suppress metal- π coupling between the aromatic rings and electrodes²⁵. In general the inclusion of the thermal fluctuations in theoretical investigations reveals a rich variety of phenomena on different timescales. For example in ref²⁶, by means of an approach based on combined density functional theory and molecular dynamics calculations together with transport calculations, the authors show that, thermally induced structural fluctuations of the electrodes, on time-scales of hundreds of ps, cause a modification of the conductance peaks in the conductance histograms. In particular

they show that the main effect of such structural fluctuations is more effective for disordered electrodes and consist in a sensible broadening of the conductance peaks and in a small reduction of a factor less than two.

Perhaps the most well-known manifestation of QI occurs in phenyl rings, whose electrical conductance with *meta* linkages to metal electrodes is strongly suppressed compared with the conductance in the presence of *para* linkages^{5, 19}. In these examples, the *meta* or *para*-linked ring lies in the centre of the molecule, remote from the region of contact with electrodes and the suppression in conductance occurs, because with a *meta* linkage, partial de Broglie waves traversing the two arms of the phenyl ring interfere destructively. In more complex molecules with more than one phenyl ring, it is of interest to probe how combinations of *meta* and *para* couplings affect transport through the molecule when the rings are located closer to the ends of the molecule and can interact directly with electrodes^{10, 12}. In this case, at room temperature, the phenyl rings are subject to thermal fluctuations and the resulting thermal distribution of conformations means that the position of the anchor group relative to the electrode is uncertain. This 'entropic' effect is in addition to inelastic electron-phonon scattering, which typically leads to small changes in transport properties at room temperature²⁷⁻²⁹. The aim of the present paper is to investigate the interplay between conformational fluctuations and quantum interference in such molecules and to establish the relative importance in these distinct contributions to single-molecule electron transport. A key result is that thermally-induced conformational fluctuations reduce the probability of metal- π coupling, which would otherwise tend to hide the effect of QI in aromatic anchor groups³⁰ and therefore counterintuitively, conformational fluctuations increase the effect of QI in such molecules.

Figure 1 shows a family of methylsulfide-functionalized trans- α,ω -diphenylolefin molecules, with terminal phenyl rings containing meta or para linkages. Following the notation of Ref.¹², we refer to these molecules as PPn, PMn, Pn and M1, where P or M denotes the position of the methylsulfide (-MeS) anchor groups (P=*para*, M=*meta*), and n denotes the length of the central olephin chain. If electron transport takes place only via the -MeS anchor groups and is forbidden in the absence of such groups, then transport through the meta-linked PMn molecules should be suppressed compared with the PPn molecules and there should be no transport through the Pn and M1 molecules. However such a picture is too simplistic, because at room temperature, conformational fluctuations will cause the anchor groups to sample a variety of configurations and therefore the effect of QI may be diminished. For example, molecules ending with phenyl termini can have a non-negligible conductance even in the absence of an anchor group due to metal- π coupling¹² between the terminal aromatic ring and the gold electrode. If fluctuations increase the probability of π -metal coupling, then the para-versus-meta location of the -MeS group should not be so crucial, since π -metal coupling may provide a parallel conductance path, which is independent of the position of the -MeS group.

Results and discussion

We investigated the interplay between conformational fluctuations and QI by presenting theoretical calculations of electron transport through this family of molecules, which also allowed us to interpret the experimental results of ref¹² and reveal their distinct transport regimes as a function of junction evolution. Initially we performed zero-temperature ab-initio calculations of electron transport through single-molecule gold junctions (shown in Figure S6) for a range of electrode separations. We then repeated the

calculations for an ensemble of binding configurations, obtained from room-temperature classical molecular dynamics simulations. Compared with predictions based on density functional theory (DFT) alone, the inclusion of conformational fluctuations was found to produce much closer agreement with the experiments of ref¹².

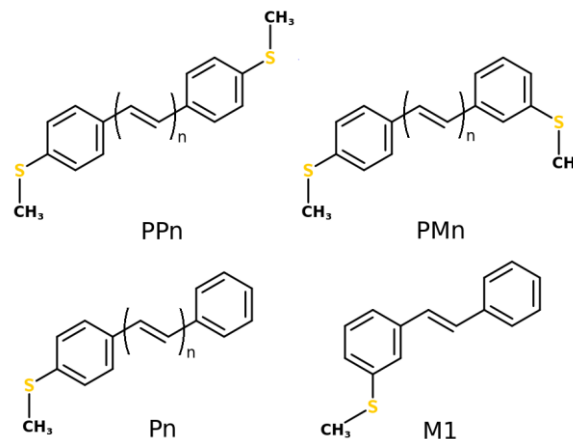


Figure 1. Four classes of molecules investigated in this paper, where $n=1,2,3$ refers to different lengths of the alkene chain between the phenyl groups. PP refers to the presence of para-para linkages of the -MeS anchor group, PM refers to the presence of para-meta linkages, P refers only one para linkage and M refers only one meta linkage in the molecule¹².

As examples, for molecules PP1 and PM1, Figure 2a shows relaxed configurations obtained from bare DFT simulations, while Figure 2b shows examples of junctions encountered during finite-temperature molecular dynamics simulations. The electrode separations (defined as the center to center distances of the apex gold atoms and denoted by x) used in these examples are indicated by black vertical lines in Figures 2c and 2d. The resulting plots of the bare DFT conductances versus electrode separation are shown as green crosses in Figures 2c and 2d respectively. For comparison, the finite temperature, conformationally-averaged conductances are plotted as red crosses. For the bare DFT conductances, the π -metal bond is the dominant channel of transmission up to $x=1.5$ nm for PP1 and $x=1.4$ nm for PM1 and over this range of separations, the conductance traces of the two molecules are similar. However beyond these separations they differ significantly, with the PP1 trace remaining rather flat between the vertical lines marked A and B, while the PM1 trace decreases by two orders of magnitude. This difference reflects the fact that at these larger separations, the metal- π bond becomes gradually less relevant and the conductance becomes dominated by the -MeS anchor-electrode bond. Beyond the vertical lines B, both conductance traces decrease rapidly as the junction breaks.

As shown in Figure S1 of the S.I., the above behaviour is a common feature of all PPn and PMn molecules for $n=1,2$ and 3. Closer inspection of the geometries during the crossover from π -metal- to anchor-metal-dominated transport reveals that the transition takes place in two stages. In the first stage, one of the electrodes switches from π -metal to anchor-metal coupling, while the other retains its π -metal character, because the simultaneous switching of both contacts is highly improbable. This switching, as shown by the geometries in the top rows of Figure 2a, occurs at $x=1.0$ nm in Figure 2c and $x=1.1$ nm in Figure 2d and accounts for the main jump in conductance, before the onset of the plateaus. The second electrode switches from π -metal to anchor-metal conductance at around $x=1.5$ nm in Figure 2c and $x=1.4$ nm in Figure 2d and does not produce a large jump in conductance. Figure S1 of the SI also

reveals that the traces of Pn (Mn) molecules possess the same qualitative features as PPn (PMn) molecules, but break at smaller values of the electrode separation.

In the case of the Pn molecules the experimental conductance may have contributions from $\pi - \pi$ stacked molecules as well that we did not consider in this study.

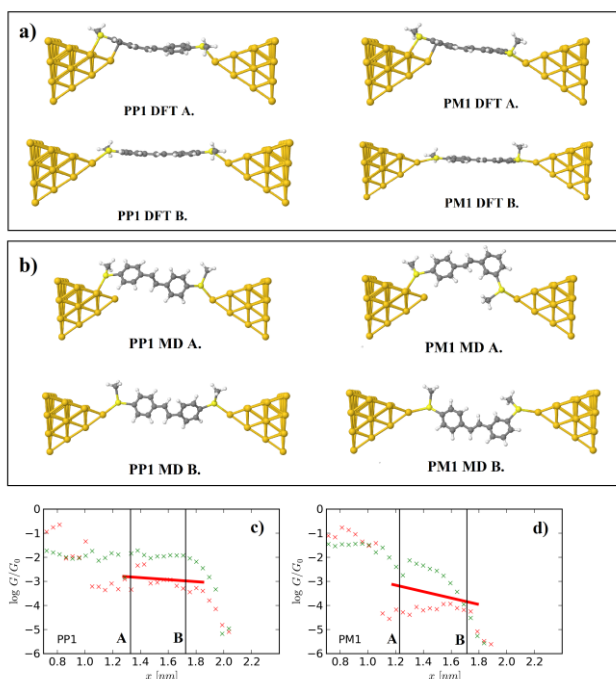


Figure 2. a) Two relaxed structures obtained from bare DFT calculations, for the PP1 molecule (left junctions) and the PM1 molecule (right junctions). For configurations PP1 DFT A and PM1 DFT A, the π -metal coupling is present. b) Two structures of PP1 and PM1 obtained using classical MD calculations. For configurations PP1 MD A and PM1 MD A there is no π -metal coupling. The green crosses in panels c) and d) show the DFT calculated conductance traces, while the red crosses show conformationally-averaged conductances calculated from snapshots obtained using molecular dynamics. The red lines show the averaged experimental traces. The vertical black lines mark the electrode separations of configurations A and B in Figures 2a and 2b.

The effect of conformational entropy is illustrated by the ensemble-averaged conductances plotted as red crosses in Figures 2c and 2d. In this case, a transition from the higher π -metal conductances occurs at the much smaller separations of approximately $x = 1.0$ nm for both PP1 and PM1, after which both molecules possess flat plateaus up to the position of vertical line B. The plateau conductance of PM1 is an order of magnitude lower than that of PP1, reflecting the significance of their meta versus para couplings and therefore we conclude that signatures of destructive versus constructive interference survive when conformational fluctuations are included. A striking feature of both molecules is that in the plateau regions between the vertical black lines, fluctuations lead to at least an order of magnitude reduction in the conductance compared with the bare DFT prediction.

To compare with experiments, the red solid lines in Figures 2c and 2d, show the experimental traces reported in ref¹². For PP1 there is close agreement with the ensemble-averaged conductances (red crosses) while for PM1, the experimental result lies between the bare-DFT and the ensemble-averaged conductances. To compare our results with experimental values over the whole family of molecules shown in Figure 1., we calculated the average of the log of the theoretical conductances for the different junctions in the separation range x_0 to x_1 where $x_1 - x_0$ is the experimental step-length¹² and x_1 is the breaking separation in DFT simulations. Figure 3 shows a comparison between these values and the experimental results. This comparison shows that the inclusion of fluctuations (yellow plot) produces a significant improvement in the agreement with experiment (blue plot) compared with the bare-DFT predictions (red plot).

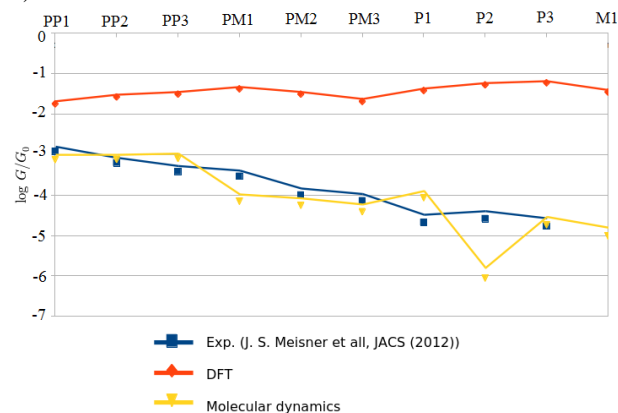


Figure 3. Comparison between the experimental conductances (blue squares) and theoretical conductances obtained from bare DFT (orange triangles) and from ensembles averages obtained using molecular dynamics (yellow triangles). The lines are guides for the eye.

It also demonstrates the crucial interplay between QI and conformational entropy in determining the measured conductances in ref¹². Bare DFT (orange line) disagrees with experiment (blue line) whereas, the inclusion of entropic effects via molecular dynamics calculations yields good agreement with the experimental conductances. Systematic comparison of conductance measurements and bare-DFT based calculations for toluene molecules³¹ and oligoynes³² with various anchors led to the conclusion that even after Fermi energy correction, bare DFT theoretical conductances were typically an order of magnitude larger than measured values. Our present study shows that one possible and significant contribution to this discrepancy is configurational entropy.

Methods

First we calculated the optimal relaxed molecular structures of the molecules M1, Pn, PMn, PPn using the SIESTA^{33, 34} implementation of density functional theory (DFT). In the DFT calculations we used the DZP localized basis set, the Generalized Gradient Approximation (GGA) with PBE parameterization and 300 Ry grid cutoff. The force tolerance for the geometrical relaxation was 0.01 eV/Å. To simulate the elongation processes of the junctions, the resulting optimal molecular geometries were sandwiched between two opposing [111] directed gold pyramids of 20 atoms with different separations of the pyramids. The separation x of the electrodes is defined as the distance between the center of the two

apex gold atoms (shown in Figure S2). The molecule was placed approximately midway in between the gold pyramids and to avoid spurious symmetries was initially located 0.5 Å closer to one of the pyramids. For electrode separations shorter than the molecular lengths, the phenyl rings lay co-facially on the gold pyramids surfaces. The shortest initial separation was about 7 Å shorter than the molecular lengths¹² to allow the development of clear π -gold overlap. Subsequent junction geometries were generated with increasing separations with increments of 0.5 Å. For every molecule, we generated 30 electrode separations and for all such steps we performed geometry optimization that involved fixing the two outer layers of the left and right pyramids, while allowing the four gold atoms closest to the tip to relax. Examples of relaxed geometries are shown in Figure 2a.

In order to calculate the electron transport properties of these junctions using DFT, we calculated the self-consistent, mean-field Hamiltonian of the junctions at each electrode separation, using the DFT code SIESTA^{33, 34}. To calculate the transmission coefficient $T(E)$ for electrons of energy E traversing the junction, we then used the wide-band approximation, which approximates the self-energy of the electrode by $\Sigma_{L(R)} \approx \Gamma S_{L(R)}$ where $\Gamma = 4eV$ and $S_{L(R)}$ are the block of the orbital overlap matrix belonging to the outermost layers of the left(right) gold pyramid (see Ref.³⁵). At each electrode separation, the electron transmission coefficient $T(E)$ was used to calculate the conductance G via the Landauer formula $G = (2e^2/h) \int dE T(E) (-df(E))/dE$, where $f(E)$ is the Fermi function $f(E) = 1/(\exp(E-E_F)/k_B T + 1)$, evaluated using the Fermi energy E_F obtained from SIESTA.

In order to investigate the effect of conformational entropy, we performed molecular dynamics simulations for each electrode separation, using LAMMPS³⁶, with the reaxFF force-field described in³⁷⁻⁴⁰ and a Nosé–Hoover NVT thermostat at $T=300K$. During the simulations, the molecules were allowed to fluctuate, whereas the gold and sulfur atoms were held fixed (Figure 2b). As initial conditions for the molecular dynamics calculations we used the DFT relaxed structures of the junctions obtained using SIESTA. Before initiating the time development, the junction structures were further optimized using the reaxFF force-field. This did not result in a major rearrangement of the geometry and only caused minor bond length changes. One exception was the Pn molecules, which even for electrode separations smaller than the molecular length, were found to detach from the gold electrode on the side without an anchor group. For each electrode separation, we first ran a 5ps long time evolution. We then continued the simulation for 50ps and recorded frames at every 2.5ps to obtain a total of 20 frames per electrode separation. Examples of such snapshots are shown in Figure 2b. The conductance of each frame was then calculated in the same way as for the DFT relaxed junction geometries. Since experimentally-measured conductances are time averages over many such configurations, we calculated the ensemble average of the conductances obtained for the 20 configurations at each electrode separation.

Conclusions

We studied electronic transport in four classes of single molecule junctions. We found that at small electrode separations, electron transfer due to the metal- π coupling is significant and the difference in conductance between molecules with meta and para couplings is suppressed. As the electrode separation is increased, there is a transition from metal- π coupling to anchor group-metal coupling, which in a bare DFT calculation leads to a suppression of conductance in the meta case, due to destructive quantum

interference. When conformational fluctuations are included via finite-temperature molecular dynamics, the conductance traces show a transition from metal- π to anchor-metal coupling at smaller electrode separations, after which the difference between meta and para couplings leads to a much lower conductance in the former. Therefore we conclude that configurational entropy does not destroy the signatures of destructive versus constructive interference in these molecules. At first sight, the persistence of signatures of QI is remarkable, because at these intermediate separations the conformational entropy is larger than at smaller separations. For example, in the case of a molecule able to sample N conformations labelled $i=1, \dots, N$ with probabilities P_i , the entropy S is given by $S = -\sum_i P_i \log P_i$. When the Ppn and PMn junctions are compressed, the binding energy between the phenyl rings and the gold is larger than $k_B T$ (room temperature) and therefore the number N of accessible conformations is smaller than at intermediate separations and S is reduced. For junctions with intermediate separations, the π -metal coupling becomes weaker and the molecule accesses a much larger portion of the phase space, thereby maximizing S and minimizing the Helmholtz free energy. However, since most of these configurations have broken π -metal bonds and are attached to the gold only through the anchor groups, most conductances are sensitive to the presence of meta- versus para- couplings and hence to quantum interference.

Acknowledgements

This work is supported by the UK EPSRC and the EU ITN MOLESCO.

Notes and references

^a Department of Physics and Astronomy, Uppsala University, Box 516, S-75120 Uppsala, Sweden

^b Department of Physics, Lancaster University, Lancaster LA1 4YB, United Kingdom ^c Address here.

† Authors contributed equally.

Electronic Supplementary Information (ESI) available. See DOI: 10.1039/b000000x/

1. M. Magoga and C. Joachim, *Physical Review B*, 1999, **59**, 16011.
2. L. Venkataraman, J. E. Klare, C. Nuckolls, M. S. Hybertsen and M. L. Steigerwald, *Nature*, 2006, **442**, 904-907.
3. G. J. Ashwell, P. Wierchowicz, L. J. Phillips, C. J. Collins, J. Gigon, B. J. Robinson, C. M. Finch, I. R. Grace, C. J. Lambert and P. D. Buckle, *Physical Chemistry Chemical Physics*, 2008, **10**, 1859-1866.
4. A. Mishchenko, D. Vonlanthen, V. Meded, M. Burkle, C. Li, I. V. Pobelov, A. Bagrets, J. K. Viljas, F. Pauly and F. Evers, *Nano Letters*, 2009, **10**, 156-163.
5. M. Taniguchi, M. Tsutsui, R. Mogi, T. Sugawara, Y. Tsuji, K. Yoshizawa and T. Kawai, *Journal of the American Chemical Society*, 2011, **133**, 11426-11429.
6. W. Hong, H. Valkenier, G. Mészáros, D. Z. Manrique, A. Mishchenko, A. Putz, P. M. García, C. J. Lambert, J. C. Hummelen and T. Wandlowski, *Beilstein Journal of Nanotechnology*, 2011, **2**, 699-713.
7. C. M. Guédon, H. Valkenier, T. Markussen, K. S. Thygesen, J. C. Hummelen and S. J. van der Molen, *Nature Nanotechnology*, 2012, **7**, 305-309.

8. H. Vazquez, R. Skouta, S. Schneebeli, M. Kamenetska, R. Breslow, L. Venkataraman and M. S. Hybertsen, *Nature Nanotechnology*, 2012, **7**, 663-667.
9. S. Ballmann, R. Härtle, P. B. Coto, M. Elbing, M. Mayor, M. R. Bryce, M. Thoss and H. B. Weber, *Physical Review Letters*, 2012, **109**, 056801.
10. S. V. Aradhya, J. S. Meisner, M. Krikorian, S. Ahn, R. Parameswaran, M. L. Steigerwald, C. Nuckolls and L. Venkataraman, *Nano Letters*, 2012, **12**, 1643-1647.
11. V. Kaliginedi, P. Moreno-García, H. Valkenier, W. Hong, V. M. García-Suárez, P. Buitter, J. L. H. Otten, J. C. Hummelen, C. J. Lambert and T. Wandlowski, *Journal of the American Chemical Society*, 2012, **134**, 5262-5275.
12. J. S. Meisner, S. Ahn, S. V. Aradhya, M. Krikorian, R. Parameswaran, M. Steigerwald, L. Venkataraman and C. Nuckolls, *Journal of the American Chemical Society*, 2012, **134**, 20440-20445.
13. C. M. Finch, V. M. García-Suarez and C. J. Lambert, *Physical Review B*, 2009, **79**, 033405.
14. C. Evangeli, K. Gillemot, E. Leary, M. T. González, G. Rubio-Bollinger, C. J. Lambert and N. Agrait, *Nano Letters*, 2013, **13**, 2141-2145.
15. C. R. Arroyo, R. Frisenda, K. Moth-Poulsen, J. S. Seldenthuis, T. Bjørnholm and H. S. J. van der Zant, *Nanoscale Research Letters*, 2013, **8**, 1-6.
16. C. M. Finch, S. Sirichantaropass, S. W. Bailey, I. M. Grace, V. M. García-Suárez and C. J. Lambert, *Journal of Physics: Condensed Matter*, 2008, **20**, 022203.
17. T. A. Papadopoulos, I. M. Grace and C. J. Lambert, *Physical Review B*, 2006, **74**, 193306.
18. E. J. Dell, B. Capozzi, K. H. DuBay, T. C. Berkelbach, J. R. Moreno, D. R. Reichman, L. Venkataraman and L. M. Campos, *Journal of the American Chemical Society*, 2013, **135**, 11724-11727.
19. R. E. Sparks, V. M. García-Suárez, D. Z. Manrique and C. J. Lambert, *Physical Review B*, 2011, **83**, 075437.
20. H. Basch, R. Cohen and M. A. Ratner, *Nano Letters*, 2005, **5**, 1668-1675.
21. D. Q. Andrews, R. P. Van Duyne and M. A. Ratner, *Nano Letters*, 2008, **8**, 1120-1126.
22. C. Li, I. Pobelov, T. Wandlowski, A. Bagrets, A. Arnold and F. Evers, *Journal of the American Chemical Society*, 2007, **130**, 318-326.
23. X. Li, J. He, J. Hihath, B. Xu, S. M. Lindsay and N. Tao, *Journal of the American Chemical Society*, 2006, **128**, 2135-2141.
24. M. Paulsson, C. Krag, T. Frederiksen and M. Brandbyge, *Nano Letters*, 2008, **9**, 117-121.
25. S. Y. Quek, M. Kamenetska, M. L. Steigerwald, H. J. Choi, S. G. Louie, M. S. Hybertsen, J. B. Neaton and L. Venkataraman, *Nature Nanotechnology*, 2009, **4**, 230-234.
26. W. R. French, C. R. Iacovella, I. Rungger, A. M. Souza, S. Sanvito and P. T. Cummings, *The Journal of Physical Chemistry Letters*, 2013, **4**, 887-891.
27. T. Markussen and K. S. Thygesen, *Physical Review B*, 2014, **89**, 085420.
28. M. Galperin, M. A. Ratner and A. Nitzan, *Journal of Physics: Condensed Matter*, 2007, **19**, 103201.
29. T. Frederiksen, M. Paulsson, M. Brandbyge and A.-P. Jauho, *Physical Review B*, 2007, **75**, 205413.
30. C. R. Arroyo, S. Tarkuc, R. Frisenda, J. S. Seldenthuis, C. H. M. Woerde, R. Eelkema, F. C. Grozema and H. S. J. van der Zant, *Angewandte Chemie*, 2013, **125**, 3234-3237.
31. W. Hong, D. Z. Manrique, P. Moreno-García, M. Gulcur, A. Mishchenko, C. J. Lambert, M. R. Bryce and T. Wandlowski, *Journal of the American Chemical Society*, 2012, **134**, 2292-2304.
32. P. Moreno-García, M. Gulcur, D. Z. Manrique, T. Pope, W. Hong, V. Kaliginedi, C. Huang, A. S. Batsanov, M. R. Bryce and C. Lambert, *Journal of the American Chemical Society*, 2013, **135**, 12228-12240.
33. E. Artacho, E. Anglada, O. Diéguez, J. D. Gale, A. García, J. Junquera, R. M. Martin, P. Ordejón, J. M. Pruneda and D. Sánchez-Portal, *Journal of Physics: Condensed Matter*, 2008, **20**, 064208.
34. J. M. Soler, E. Artacho, J. D. Gale, A. García, J. Junquera, P. Ordejón and D. Sánchez-Portal, *Journal of Physics: Condensed Matter*, 2002, **14**, 2745.
35. C. J. O. Verzijl, J. S. Seldenthuis and J. M. Thijssen, *The Journal of Chemical Physics*, 2013, **138**, 094102.
36. S. Plimpton, *Journal of Computational Physics*, 1995, **117**, 1-19.
37. O. Rahaman, A. C. T. van Duin, W. A. Goddard Iii and D. J. Doren, *The Journal of Physical Chemistry B*, 2010, **115**, 249-261.
38. J. A. Keith, D. Fantauzzi, T. Jacob and A. C. T. van Duin, *Physical Review B*, 2010, **81**, 235404.
39. T. T. Järvi, A. C. T. van Duin, K. Nordlund and W. A. Goddard Iii, *The Journal of Physical Chemistry A*, 2011, **115**, 10315-10322.
40. G.-T. Bae and C. M. Aikens, *The Journal of Physical Chemistry A*, 2013, **117**, 10438-10446.